

**A ribosomal protein homolog governs gene expression and virulence in a bacterial  
pathogen**

Hannah S. Trautmann<sup>1</sup> and Kathryn M. Ramsey<sup>1,2,\*</sup>

<sup>1</sup>Department of Cell and Molecular Biology, University of Rhode Island, Kingston, RI 02881, USA

<sup>2</sup>Department of Biomedical and Pharmaceutical Sciences, University of Rhode Island, Kingston, RI  
02881, USA

\* To whom correspondence should be addressed: Kathryn M. Ramsey [kramsey@uri.edu](mailto:kramsey@uri.edu)

## Abstract

1           The molecular machine necessary for protein synthesis, the ribosome, is generally considered  
2   constitutively functioning and lacking any inherent regulatory capacity. Yet ribosomes are commonly  
3   heterogenous in composition and the impact of ribosome heterogeneity on translation is not well  
4   understood. Here we determine that changes in ribosome protein composition governs gene  
5   expression in the intracellular bacterial pathogen *Francisella tularensis*. *F. tularensis* encodes three  
6   distinct homologs for bS21, a ribosomal protein involved in translation initiation, and analysis of  
7   purified *F. tularensis* ribosomes reveals they are heterogenous with respect to bS21. Loss of one  
8   homolog, bS21-2, results in significant changes to the cellular proteome unlinked to changes in the  
9   transcriptome. Among the reduced proteins are components of the type VI secretion system (T6SS), an  
10   essential virulence factor encoded by the Francisella Pathogenicity Island. Furthermore, loss of bS21-2  
11   leads to an intramacrophage growth defect. Although multiple bS21 homologs complement loss of  
12   bS21-2 with respect to T6SS protein abundance, bS21-2 is uniquely necessary for robust  
13   intramacrophage growth, suggesting bS21-2 modulates additional virulence gene(s) distinct from the  
14   T6SS. Our results indicate that ribosome composition in *F. tularensis*, either directly or indirectly, post-  
15   transcriptionally modulates gene expression and virulence. Our findings are consistent with a model in  
16   which bS21 homologs function as post-transcriptional regulators, allowing preferential translation of  
17   specific subsets of mRNAs, likely at the stage of translation initiation. This work also raises the  
18   possibility that bS21 in other organisms may function similarly and that ribosome heterogeneity may  
19   permit many bacteria to post-transcriptionally regulate gene expression.

## 20 **Importance**

21           While bacterial ribosomes are commonly heterogenous in composition (e.g., incorporating  
22 different homologs for a ribosomal protein), how heterogeneity impacts translation is unclear. We  
23 found that the intracellular human pathogen *Francisella tularensis* has heterogenous ribosomes,  
24 incorporating one of three homologs for ribosomal protein bS21. Furthermore, one bS21 homolog  
25 post-transcriptionally governs expression of the *F. tularensis* type VI secretion system, an essential  
26 virulence factor. This bS21 homolog is also uniquely important for robust intracellular growth. Our data  
27 support a model in which bS21 heterogeneity leads to modulation of translation, providing another  
28 source of post-transcriptional gene regulation. Regulation of translation by bS21, or other sources of  
29 ribosomal heterogeneity, may be a conserved mechanism to control gene expression across the  
30 bacterial phylogeny.

## 31 Introduction

32 Regulation of translation provides bacteria with a rapid way to modify gene expression. While  
33 many distinct mechanisms permit this fine-tuning (1, 2) the impact of ribosome composition on gene  
34 expression remains poorly-understood. In bacteria, ribosomes are diverse and commonly  
35 heterogenous with respect to ribosomal protein (r-protein) content, post-translational modifications,  
36 rRNA content, or post-transcriptional modifications (reviewed in (3)). The functional consequences of  
37 ribosome heterogeneity are unclear but may include the formation of “specialized ribosomes,” or  
38 ribosomes with altered activity due to their distinct composition (4). Although specialized ribosomes  
39 are not well described in bacteria, exciting recent studies have connected altered rRNA content of  
40 ribosomes and gene regulation (5, 6) and, in *Mycobacterium smegmatis*, ribosomes containing  
41 alternate r-protein homologs translate some genes with differential efficiency (7).

42 *Francisella tularensis* is a Gram-negative, facultative intracellular bacterium that causes the  
43 potentially fatal human disease tularemia (8). After internalization into host cells, *F. tularensis* must  
44 escape from the Francisella-containing phagosome to replicate inside the cytosol. This escape process  
45 requires a type VI secretion system (T6SS), which modifies the host cell by delivery of effector proteins  
46 (9–12). Production of this T6SS is coordinately regulated by the transcription factors MglA, SspA, and  
47 PigR, as well as the signaling molecule ppGpp (13–20). Regulation of the T6SS is arguably the most  
48 well-understood virulence regulatory network in *F. tularensis*. However, much remains to be learned  
49 about the regulation of other virulence factors.

50 Despite its relatively small genome (< 2 Mbp), *F. tularensis* encodes three distinct *rpsU* genes  
51 (*rpsU1*, *rpsU2*, and *rpsU3*), which encode homologs of the small ribosomal subunit protein bS21 (bS21-  
52 1, bS21-2, and bS21-3, respectively). This is the only apparent source of ribosome heterogeneity in *F.*

53 *tularensis*, as the three rRNA operon sequences are identical and no other r-proteins are encoded by  
54 multiple homologs. In *Escherichia coli*, bS21 is involved in translation initiation (21, 22) and, consistent  
55 with this activity, is found on the ribosome close to the anti-Shine-Dalgarno sequence near the mRNA  
56 exit channel (23, 24). Furthermore, bS21 is one of the last r-proteins to assemble into the ribosome, is  
57 considered “loosely associated,” and is easily exchanged among assembled ribosomes (25, 26).

58       Using mass spectrometry and immunoblot analyses, we show that ribosomes in *F. tularensis* are  
59 heterogenous with respect to bS21 content and can incorporate any of the three bS21 homologs into  
60 actively-translating ribosomes. Using quantitative whole-cell proteomics, quantitative immunoblots,  
61 and transcriptomic analyses, we demonstrate that loss of a particular bS21 homolog, bS21-2, leads to  
62 changes in abundance for a subset of proteins that cannot be explained by changes in transcript  
63 abundance. Among the impacted proteins are multiple virulence factors, including those that comprise  
64 the T6SS. Finally, using intramacrophage growth assays, we provide evidence that bS21-2, and not the  
65 other bS21 homologs, promotes intramacrophage growth. Our findings reveal that a specific r-protein  
66 homolog in *F. tularensis*, bS21-2, governs gene expression at the level of protein abundance and  
67 positively impacts virulence.

68

## 69 **Results**

### 70 ***Francisella* species encode three bS21 homologs**

71       The genomes of multiple *Francisella* species contain three distinct genes encoding bS21 (*rpsU1*,  
72 *rpsU2*, and *rpsU3*), raising the possibility that cells contain ribosomes that are heterogenous with  
73 respect to bS21 content. The gene encoding one homolog in *F. tularensis*, *rpsU2* (encoding bS21-2), is

74 syntenic with the single bS21-encoding gene in *Escherichia coli* (**Figure S1**). In *E. coli*, *rpsU* is the first in  
75 an operon referred to as the macromolecular synthesis operon, encoding key proteins for initiation of  
76 translation (bS21), DNA replication (DNA primase), and transcription (RNA polymerase  $\sigma^{70}$ ) (27). The  
77 corresponding operon in *Francisella* species, including *F. tularensis*, also contains *yqeY*, which may  
78 encode a protein necessary for correct tRNA aminoacylation (28). Another bS21 homolog, bS21-1, is  
79 encoded by *rpsU1* in an apparent operon downstream of the gene for cold shock protein CspC. There  
80 are no annotated genes in the same transcriptional context as *rpsU3*, the gene encoding the third  
81 homolog, bS21-3. The bS21 homologs in *F. tularensis* are distinct but similar, with amino acid identities  
82 ranging from 48 – 72%, and are similar to *E. coli* bS21 (51 – 60% identical, with bS21-2 having the  
83 highest identity; **Figure S2**).

#### 84 ***F. tularensis* ribosomes are heterogenous**

85 The presence of three distinct genes encoding bS21 raises the potential for *F. tularensis*  
86 ribosomes to be heterogenous with respect to bS21. To investigate this possibility, we used sucrose  
87 cushion centrifugation to isolate ribosomes from *F. tularensis* LVS grown *in vitro* in quadruplicate and  
88 analyzed their protein composition using liquid chromatography tandem mass spectrometry (LC-  
89 MS/MS). Approximately 80% of the spectral counts corresponded to ribosomal proteins or proteins  
90 associated with transcription and translation complexes (e.g., RNA polymerase, translation release  
91 factors, SRP), indicating *F. tularensis* ribosomes purified in this manner are highly pure (**Figure 1A**,  
92 **Table S1**). Despite the small size of bS21 (approx. 8 kDa), we identified multiple peptides corresponding  
93 to bS21-2 in all samples. In one sample, peptides shared between bS21-1 and bS21-3 were detected  
94 (**Figure 1B**). This suggests that bS21-2 is the most abundant homolog in wild-type cells, consistent with

95 its production from an operon encoding proteins essential for transcription and DNA replication. It also  
96 suggests that either bS21-1, bS21-3, or both, are incorporated into ribosomes in LVS. However, it did  
97 not allow us to determine the next-most abundant homolog (bS21-1 or bS21-3) or confirm  
98 incorporation of both of these other homologs. Regardless, these results demonstrate that multiple  
99 bS21 homologs are incorporated into wild-type *F. tularensis* ribosomes and that ribosomes in *F.*  
100 *tularensis* are heterogenous, containing different bS21 homologs.

101 We next wanted to determine if each bS21 homolog can be found in actively-translating  
102 ribosomes. To track each bS21, we modified each homolog to encode a C-terminal vesicular stomatitis  
103 virus glycoprotein (VSV-G) tag and individually ectopically expressed them, using the same promoter,  
104 from a plasmid in wild-type cells. Lysate fractions of these cells were analyzed by immunoblotting after  
105 sucrose gradient sedimentation (**Figure 1C; Figure S3**). When ectopically expressed (rather than  
106 produced from its native locus), bS21-1 was the least abundant homolog while bS21-3 was produced at  
107 the highest level. Each homolog was found in fractions corresponding to the 30S, 70S, and polysomes.  
108 Although bS21 is thought to function primarily in translation initiation, our findings indicate that each  
109 bS21 homolog associates with the ribosome throughout the translation cycle.

#### 110 ***Loss of bS21-2 leads to changes in protein, not transcript, abundance***

111 Because the ribosomal protein bS21 is involved in translation initiation, we hypothesized that  
112 loss of a bS21 homolog may impact translation and result in changes in abundance in a subset of  
113 proteins. To test this hypothesis, we individually deleted each of the three genes encoding bS21  
114 homologs. This led us to determine that no single bS21 homolog is essential for cell growth. We  
115 subsequently grew wild-type cells and cells lacking single bS21 homologs to mid-log *in vitro* and used

116 data-independent acquisition (DIA) mass spectrometry analysis (29) to compare relative protein  
117 abundance in cell lysates. Using this method, 68% of the total proteins predicted to be encoded by *F.*  
118 *tularensis* LVS were identified and analyzed (1194 of 1754). When compared to wild-type, we did not  
119 detect any significant changes in protein abundance in cells lacking either of the two lower-abundance  
120 bS21 homologs, bS21-1 and bS21-3 (>1.5-fold altered with an adjusted p-value <0.05, excluding bS21).  
121 In contrast, cells lacking the most abundant homolog, bS21-2 ( $\Delta rpsU2$ ), had significant proteomic  
122 differences compared to wild-type cells. Specifically, we found 185 unique proteins (~16% of detected  
123 proteins) had altered abundance in cells without bS21-2 compared to wild-type cells (**Figure 2**, data on  
124 y-axis, **Table S2**).

125 To determine if these changes in protein abundance can be explained by corresponding  
126 changes in transcription, we performed transcriptomic analyses on wild-type cells, cells lacking bS21-2  
127 ( $\Delta rpsU2$ ), and cells lacking the native bS21-2 but ectopically expressing bS21-2-V from a plasmid.  
128 Comparing cells with and without native bS21-2, we identified 105 differentially expressed genes (>2-  
129 fold altered with an adjusted p-value <0.05, excluding *rpsU*; **Figure 2**, data on x-axis, **Table S3**). All of  
130 these changes were complemented by ectopic expression of bS21-2-V on a plasmid.

131 Our analysis revealed that in cells lacking bS21-2, the largest change in transcript abundance  
132 was a six-fold increase in *yqeY*, the gene directly downstream from *rpsU2* (which encodes bS21-2). This  
133 increase in transcript abundance was complemented by ectopic expression of bS21-2-V, suggesting  
134 that bS21-2 functions as a negative regulator of its own operon. Translational feedback regulation is  
135 well-established for multiple ribosomal proteins but, to the best of our knowledge, this is the first



136 report of translational regulation of ribosomal proteins in *F. tularensis* and the first report that bS21  
137 governs its own production (30, 31).

138         Comparison of our proteomic and transcriptomic analyses reveals that the changes in protein  
139 abundance were not generally due to changes in transcript abundance. Of the 185 differentially  
140 abundant proteins in cells lacking bS21-2, only ~12% (23) could be explained by altered transcription  
141 (**Figure 2**, yellow dots), while about 88% (162; **Figure 2**, blue dots and orange dot) had changes in  
142 protein abundance without a corresponding change in transcript abundance. These discrepancies  
143 between transcript abundance and protein abundance support a model in which bS21-2 controls  
144 expression, either directly or indirectly, of some genes at the level of translation.

145 ***bS21-2 governs the abundance of type VI secretion system proteins, which are essential for virulence***

146         Among the proteins with altered abundance in cells lacking bS21-2, we identified twelve out of  
147 sixteen proteins encoded on the Francisella pathogenicity island (FPI). The FPI encodes a unique type VI  
148 secretion system (T6SS) that is absolutely essential for intramacrophage growth and virulence of  
149 *F. tularensis* (32–34). Using quantitative immunoblotting and antibodies specific to a subset of  
150 *F. tularensis* T6SS proteins, we validated that cells lacking bS21-2 have differences in those T6SS  
151 proteins (**Figure 3**). Consistent with the mass spectrometry results, we found reductions in virtually all  
152 probed T6SS proteins, including an ~4-fold reduction in PdpB, the TssM/IcmF homolog. Using this  
153 approach, we also found an ~2.4-fold reduction in IgIA and ~1.7-fold reduction in IgIB, T6SS proteins  
154 that are just below the cutoff for statistical significance in our mass spectrometry analysis. Since we  
155 identified this differential abundance using a more sensitive method of comparison, it raises the  
156 possibility that all FPI-encoded proteins may be differentially abundant in cells lacking bS21-2

157 compared to wild-type cells, but we do not have antibodies specific to the remaining proteins (i.e.,  
158 PdpE and VgrG) to test this hypothesis. Also consistent with our mass spectrometry findings, IgID (the  
159 homolog of TssK) was the only T6SS protein with increased, rather than decreased, protein abundance  
160 (**Figure 3**). Each of these changes in protein abundance could be complemented by ectopic expression  
161 of bS21-2-V, driven by the *groES* promoter on a plasmid (**Figure 3**).

162         These changes in protein abundance likely reflect positive regulation of most, but not all, T6SS  
163 proteins by bS21-2 at the level of translation, either directly or indirectly. Our findings are inconsistent  
164 with bS21 positively regulating transcription; it is well-established that transcription of FPI operons are  
165 coordinately controlled and our RNA-Seq analysis reveals that cells lacking bS21-2 do not have FPI-wide  
166 transcript reductions (13–16, 20, 35); **Table S3**). In a complementary approach, we compared the  
167 transcript abundance for specific FPI genes using quantitative RT-PCR and included cells lacking PigR, a  
168 transcription factor critical for positive transcriptional regulation of FPI genes (14–16, 20, 35); **Figure**  
169 **S4**). We confirmed that cells lacking PigR have major decreases in FPI transcript abundance but cells  
170 lacking bS21-2 did not have compelling (2-fold or greater) changes in FPI transcript abundance or in  
171 transcript abundance of the positive regulator PigR, consistent with the RNA-Seq results. We  
172 considered the possibility that loss of bS21-2 could indirectly impact T6SS protein abundance by  
173 altering protein stability, but the half-life of one of the most differentially abundant proteins, PdpB,  
174 was unchanged in cells with and without bS21-2 (longer than 120 minutes, **Figure S5**). Our results are  
175 consistent with bS21-2 controlling expression of T6SS proteins at the level of translation.

176 ***Other bS21 homologs impact the abundance of type VI secretion system proteins***

177 Our findings indicate that bS21-2 is the most abundant bS21 homolog in wild-type cells.  
178 However, it is not clear if the majority of ribosomes in cells lacking bS21-2 incorporate another bS21  
179 homolog or no bS21 at all. This leads to the question: do all bS21 homologs affect T6SS protein  
180 translation or does bS21-2 specifically modulate translation of T6SS proteins? To answer this question,  
181 we ectopically expressed either bS21-1-V or bS21-3-V in cells lacking bS21-2, similarly to the ectopic  
182 expression of bS21-2-V. We subsequently used quantitative immunoblot analyses to assess the  
183 abundance of each ectopically expressed bS21 homolog and a subset of T6SS proteins (**Figure 3**). While  
184 this strategy resulted in comparable amounts of bS21-2 and bS21-3, ectopic expression resulted in  
185 approximately 2-fold less bS21-1 than the other homologs, consistent with its lower expression in wild-  
186 type cells (**Figure 3, Figure 1**). With respect to T6SS protein abundance, ectopic expression of bS21-3  
187 restored all probed proteins to wild-type levels, complementing the loss of bS21-2 (**Figure 3**). However,  
188 bS21-1 did not appear to complement T6SS protein production completely (**Figure 3**). This may be due  
189 to reduced levels of bS21-1, lack of specific ability to regulate T6SS proteins, or a combination of the  
190 two factors. Notably, loss of bS21-2 resulted in a growth defect (**Table S4**) that could be complemented  
191 by ectopic expression of bS21-2 or bS21-1, but not bS21-3. That cells lacking bS21-2 with ectopic  
192 expression of bS21-3 have wild-type levels of T6SS proteins and yet still have a growth defect reveals  
193 that changes in T6SS proteins are not due simply to changes in growth rate. Our findings allow us to  
194 conclude that incorporation of either bS21-2 or bS21-3 – and to a lesser extent, bS21-1 – into  
195 ribosomes modulates production of T6SS proteins.

196 ***bS21-2 is important for intramacrophage growth***

197 A functional T6SS is essential for *F. tularensis* intramacrophage replication and is a strict  
198 requirement for virulence (32–34). The observed differences in FPI protein abundance led us to  
199 hypothesize that T6SS function may be compromised in cells lacking bS21-2 and these cells may be  
200 attenuated for intramacrophage growth. We tested the ability of cells lacking bS21-2 ( $\Delta rpsU2$ ) to  
201 survive in murine macrophage-like J774A.1 cells. This revealed a significant defect in the ability of  
202 bS21-2 mutant cells to replicate in macrophage; we recovered ten-fold fewer bS21-2 mutant bacteria  
203 after 24 hours compared to wild-type (**Figure 4**). The intramacrophage growth defect of cells lacking  
204 bS21-2 could be restored by ectopic expression of bS21-2 from a plasmid (**Figure 4**). This is in contrast  
205 to ectopic expression of bS21-1 and bS21-3, neither of which restored the intramacrophage growth of  
206 cells lacking bS21-2 (**Figure 4**). These results indicate that bS21-2 is specifically required for  
207 intramacrophage survival, despite the fact that ectopic expression of bS21-1 restored *in vitro* growth  
208 rates and ectopic expression of bS21-3 restored T6SS protein production *in vitro* (**Figure 3, Table S4**).

209 In summary, only the presence of bS21-2, not bS21-1 or bS21-3, could restore the  
210 intramacrophage growth defect of cells without bS21-2. This reveals that bS21-2 is critical for *F.*  
211 *tularensis* virulence and fits a model in which bS21-2 specifically regulates one or more genes  
212 necessary for intramacrophage growth in addition to T6SS genes, a topic still under investigation.

## 213 Discussion

214 The findings described here reveal that ribosome composition in *F. tularensis* is heterogenous  
215 with respect to the small ribosomal protein bS21 and that this heterogeneity impacts gene expression  
216 at the level of translation. In particular, by studying cells that contain ribosomes either with or without  
217 one of the three bS21 homologs, we have identified that bS21-2 governs the abundance of most T6SS

218 proteins. Additionally, cells lacking bS21-2 are defective for intramacrophage growth; since this defect  
219 can only be complemented by bS21-2, even though bS21-3 and (to a lesser extent) bS21-1 can restore  
220 T6SS protein abundance, this intramacrophage growth defect is likely independent of the impact bS21-  
221 2 has on the T6SS. This allows us to conclude that bS21-2 is important for intramacrophage growth of  
222 *F. tularensis*, potentially by regulating the translation of one or more proteins (in addition to the T6SS)  
223 necessary for virulence.

224 To examine the impact of bS21 homologs on gene expression, we used tools that assess the  
225 steady-state abundance of protein and transcripts: mass spectrometry and RNA-Seq, respectively. Our  
226 analyses revealed that when compared to wild-type cells, cells lacking bS21-2 have changes in protein  
227 abundance that cannot be explained by steady-state changes in corresponding mRNAs. Yet for some  
228 proteins with altered abundance in cells lacking bS21-2, there are corresponding modest differences in  
229 transcript abundance that do not reach statistical significance (**Figure 2**, yellow dots). It is possible that  
230 loss of bS21-2 leads to modest transcript abundance changes that result in more significant changes in  
231 protein abundance. But given the role of bS21 in translation, and specifically translation initiation, we  
232 propose a model in which bS21-2 impacts gene expression by modulating translation initiation for  
233 particular mRNAs. Since an mRNA can be stabilized by translation, increased translation can increase  
234 stability and, conversely, less translation can lead to faster degradation (reviewed in 36); this effect  
235 may impact the abundance of many transcripts in cells lacking bS21-2 and may explain the observed  
236 weak correlation between some protein and transcript abundances. Consequently, additional work will  
237 be required to validate our model.

238 Our approach in studying bS21 homologs in *F. tularensis* has thus far focused on the homolog  
239 bS21-2, whose loss led to phenotypic changes. Our data suggest that bS21-2 is the most abundant  
240 homolog in the conditions studied. We hypothesize that cells without bS21-1 and bS21-3 did not  
241 exhibit distinct phenotypes under the conditions of our experiments due to their relatively low  
242 abundance. Both of these homologs may also influence gene expression under conditions when they  
243 are more abundant, but these conditions are not yet identified. Additionally, in our study of cells  
244 without bS21-2, it is not clear if the majority of ribosomes lack bS21 entirely or instead incorporate  
245 bS21-1 or bS21-3; our findings only extend to heterogeneity with respect to the presence or absence of  
246 bS21-2.

247 Comparison of *rpsU* genes across the bacterial phylogeny reveals that many clades and species  
248 do not encode bS21, suggesting that it is not essential for translation (37, 38). However, targeted  
249 deletion of the single *rpsU* gene in *E. coli* has not been successful, suggesting bS21 is essential in *E. coli*  
250 (39–41). We reported in previous work that the *F. tularensis* homolog syntenic with *E. coli rpsU*, *rpsU2*,  
251 is essential *in vitro* using transposon-insertion sequencing (Tn-Seq) (42). Yet using a targeted allelic  
252 exchange approach, we have been able to successfully delete each *rpsU* homolog individually,  
253 indicating that none of the *F. tularensis* bS21 homologs is individually essential. Our identification of  
254 *rpsU2* as an essential gene was likely due to the polar effects of transposon insertion into the first gene  
255 of an operon containing other known essential genes (*dnaG*, encoding primase, and *rpoD*, encoding the  
256  $\sigma^{70}$  subunit of RNA polymerase). It is unclear if *F. tularensis* cells lacking all three *rpsU* genes are viable.

257 The literature reflects that bS21 may regulate gene expression in other bacteria. A recent study  
258 of the *Flavobacterium johnsoniae* ribosome revealed that bS21 plays a role in sequestering the anti-

259 Shine-Dalgarno sequence (43). This occlusion occurs through contacts with the C-terminal region of  
260 bS21 that are conserved across Bacteroidetes species and provides a rationale to explain why most  
261 Bacteroidetes mRNAs lack Shine-Dalgarno sequences. Notably, the mRNA encoding bS21 in *F.*  
262 *johnsoniae* encodes a perfect Shine-Dalgarno sequence, strongly suggesting that bS21 regulates its  
263 own expression through translational autoregulation (43). *F. tularensis*, however, is a member of the  
264 Gammaproteobacteria, has bS21 homologs that exhibit significant differences from *F. johnsoniae* at  
265 the C-terminal region, and encodes mRNAs that commonly contain sequences similar to the consensus  
266 Shine-Dalgarno sequence. This suggests that in *F. tularensis*, bS21 exerts its effects on gene expression  
267 in a different manner.

268 In other bacteria that encode it, loss of bS21 leads to a variety of phenotypic changes. In *B.*  
269 *subtilis*, loss of bS21 results in biofilm and motility defects (44) and in *Listeria monocytogenes*,  
270 inactivation of bS21 is linked to stress resistance and altered transcript abundance(45, 46).  
271 *Staphylococcus aureus* lacking functional bS21 exhibit increased resistance to the antibiotics  
272 daptomycin and vancomycin (47–49). Both *Burkholderia pseudomallei* and *F. tularensis* encode  
273 multiple bS21 homologs and in both organisms, virulence screens using transposon mutagenesis have  
274 identified one homolog as important for virulence (50, 51). Together, these findings suggest that bS21  
275 may regulate gene expression in diverse bacterial species.

276 The idea that bS21 might modulate translation for a subset of mRNAs is further supported by  
277 the recent discovery that bS21 is encoded by thousands of sequenced bacteriophage genomes and is  
278 one of the most commonly encoded phage ribosomal proteins (52, 53). Transcripts encoding bS21 have  
279 been detected in metatranscriptomic samples along with transcripts for late-stage replication proteins

280 (54) and at least one phage-encoded bS21 can be incorporated into *E. coli* ribosomes (52). All of this  
281 raises the possibility that incorporation of a viral bS21 into the host ribosome may co-opt the  
282 translation machinery in favor of viral proteins and replication.

283 Our work, together with these earlier findings, strongly suggests that incorporation of bS21 into  
284 the ribosome can impact translation of a subset of mRNAs. Considering that bS21 can easily be  
285 exchanged among ribosomes, this provides an excellent mechanism to quickly fine-tune the cellular  
286 proteome. While the molecular mechanism leading to the modulation of translation has yet to be  
287 identified, it is reasonable to speculate that bS21 impacts translation during initiation through specific  
288 interactions with the 5' untranslated regions of a specific set of mRNAs. These findings also support the  
289 idea that changes in ribosome composition may impact translation and provide another source for  
290 bacterial control of gene expression.

291

## 292 **Materials and Methods**

### 293 ***Bacterial strains and growth conditions***

294 Unless otherwise noted, bacterial strains were grown as indicated here. *Francisella tularensis* subsp.  
295 *holarctica* Live Vaccine Strain (LVS) cells were grown in Mueller-Hinton broth (BD Difco) supplemented  
296 with 0.025% iron pyrophosphate, 0.1% glucose, and 2% Isovitalex (sMHB), shaking aerobically or on  
297 cystine heart agar plates with 1% hemoglobin (CHA-H) at 37°C. *Escherichia coli* XL1-Blue cells were  
298 grown in lysogeny broth (LB) shaking aerobically or on LB agar plates at 37°C. Kanamycin was used at  
299 concentrations of 5 µg/mL (*F. tularensis*) or 50 µg/mL (*E. coli*).



300

301 **Vector construction**

302 Complementation plasmids for each bS21 homolog were created from a plasmid derived from  
303 pFNLTP6 (55), pKL42 (pF-PmrA-V). Specifically, the complementation plasmids produce bS21 homologs  
304 with a C-terminal VSV-G epitope under the control of the *F. tularensis groES* promoter. Each *rpsU* gene  
305 was amplified using a 5' primer specifying an EcoRI site and an ideal Shine-Dalgarno sequence (5'-  
306 AGGAGG-3') located six nucleotides upstream from the translation start site. The 3' primer did not  
307 include the native stop codon and included DNA specifying a NotI site. The fragment was cloned into  
308 EcoRI/NotI digested pKL42, such that the 3' end of each *rpsU* is in frame with codons specifying three  
309 alanines followed by the VSV-G epitope. The resulting plasmids were pKR6 pF-bS21-1-V, pKR7 pF-bS21-  
310 2-V, and pKR8 pF-bS21-3-V. The control plasmid pF is the original pFNLTP6 plasmid (containing the  
311 *groES* promoter but not any *rpsU* genes nor the VSV-G epitope).

312

313 The plasmid pEX18kan was modified to generate in-frame deletions of each *rpsU* gene as previously  
314 described (14). Flanking regions of ~600 base pairs from both sides of each *rpsU* gene were amplified  
315 by PCR. Primers amplifying the DNA adjacent to each *rpsU* gene included the first three or last three  
316 codons of the open reading frame and DNA specifying a NotI site, which also encodes an alanine linker  
317 (5'-GCGGCCGCT-3'). The two fragments were cloned into BamHI/KpnI-digested pEX18kan for each  
318 *rpsU* gene respectively, yielding pKL122 pEXΔ*rpsU1*, pKR11 pEXΔ*rpsU2*, and pKR12 pEXΔ*rpsU3*; these  
319 plasmids were used to construct deletions via allelic exchange as described below.

320

321 **Strain construction**

322 Deletion strains were constructed by allelic exchange as previously (56). Briefly, competent cells were  
323 made by washing *F. tularensis* LVS cells in 10% sucrose and resuspending in an equal volume of 10%  
324 sucrose to cells. At least 1 µg of allelic exchange plasmid was electroporated into 50 µL competent cells  
325 in 0.2 cm cuvettes with a 2.5 kV pulse. Cells were allowed to recover in 4 – 5 mL sMHB for 4-8 hours at  
326 37°C, shaking. Cells in which a single integration event occurred were selected for on CHA-H plates  
327 with kanamycin. These cells were subsequently plated on CHA-H containing 10% sucrose and lacking  
328 NaCl, allowing for survival only of cells that had crossed out the non-homologous portion of the vector,  
329 including *sacB* and kanamycin resistance gene. Colonies that were sucrose-resistant and kanamycin-  
330 sensitive were screened for deletions using PCR. Candidate strains were confirmed by amplification of  
331 genomic DNA outside of the flanking regions on each side of the deletion and Sanger sequencing  
332 (Rhode Island Genomics and Sequencing Center). Plasmid pKL122 pEXΔ*rpsU1* was used to make LVS  
333 Δ*rpsU1*, plasmid pRK11 pEXΔ*rpsU2* was used to make LVS Δ*rpsU2*, and plasmid pKR12 pEXΔ*rpsU3* was  
334 used to make LVS Δ*rpsU3*.

335

336 Complementation plasmids were electroporated into LVS or LVS Δ*rpsU2* cells as described above and  
337 selected for on CHA-H plates with kanamycin.

338

339 **Immunoblotting**

340 Cells were collected from mid-log cultures (OD<sub>600</sub> 0.3-0.4) and resuspended in sample loading buffer  
341 (SLB: 1X NuPAGE LDS with 50 mM DTT) normalized to OD<sub>600</sub> and heated at 95°C for 10 minutes. Cell  
342 lysates and fractions were separated by SDS-PAGE on 4-12% Bis-Tris NuPAGE gels in MES or MOPS

343 running buffer (Invitrogen) and transferred to PVDF with the Mini Blot Module transfer system  
344 (Invitrogen; 20V for 1 hour on ice) or the Criterion cell for midi gels (BioRad; 60V for 40 minutes on ice)  
345 with 1X NuPAGE transfer buffer and 10% methanol. Whole cell lysates were analyzed for total protein  
346 with the Invitrogen No-Stain Protein labeling reagent and all membranes were blocked with Odyssey  
347 blocking buffer diluted 1:5 in PBS overnight. For each antibody, the linear range of protein detection  
348 was determined by plotting sequential dilutions of one lysate from each strain as a standard curve to  
349 establish appropriate volume of lysate to load. Membranes were probed with indicated monoclonal  
350 antibodies (BEI Resources, diluted 1:1000 in blocking buffer for all antibodies except anti-PdpB, which  
351 was diluted 1:250) or the VSV-G epitope (Sigma, diluted 1:2222). Proteins were detected using IRDye  
352 800 CW donkey anti-mouse IgG or donkey anti-rabbit IgG (Li-Cor, diluted 1:10,000). Fluorescence was  
353 measured and quantified on the LiCor Odyssey CLx imager and software, and protein abundance was  
354 calculated relative to total protein in each lane. Experiments were performed at least twice in  
355 biological triplicate and two to three technical replicates.

356

### 357 ***RNA isolation and qRT-PCR***

358 Cells were collected from mid-log cultures ( $OD_{600}$  0.3-0.4). Nucleic acids were isolated using the Direct-  
359 Zol RNA purification kit (Zymo Research) according to the manufacturer's protocol. Purified nucleic  
360 acids were treated with RQ1 Dnase (Promega) for 1 hour at 37°C and RNA was purified with the Direct-  
361 Zol RNA purification kit. cDNA was synthesized using Superscript III reverse transcriptase (Life  
362 Technologies) as previously described (14). qRT-PCR was performed using PowerUp SYBR Green  
363 Master Mix (Applied Biosystems) and a Roche LightCycler 480 (University of Rhode Island Genomics  
364 and Sequencing Center) essentially as described (14). Transcript abundances of *pdpA*, *pdpB*, *iglA*, and

365 *pigR* were compared to three different control genes (*tul4*, *rpoA1*, and *bfr*) and since all results were  
366 similar, relative abundance is reported to *tul4*. Experiments comparing wild-type and *rpsU2* mutant  
367 cells were performed three times in biological triplicate; experiment with cells lacking PigR was  
368 performed once.

369

### 370 ***RNA-Seq***

371 Approximately 1.5 µg of RNA isolated as above was sent to the Microbial Genome Sequencing Center  
372 (MiGS) for RNA-Seq analysis, in biological triplicate (LVS pF) or duplicate (LVS  $\Delta rpsU2$  pF, LVS  $\Delta rpsU2$   
373 pF-bS21-2-V). After using RiboZero Plus rRNA depletion, libraries were made using Illumina Stranded  
374 RNA library preparation and sequenced for a minimum of 12 million paired end reads. Paired-end  
375 sequencing reads were mapped to the *F. tularensis* LVS genome (NCBI RefSeq accession number  
376 NC\_007880) using bowtie2 version 2.2.4. Reads that mapped to annotated genes were counted using  
377 HTSeq version 0.11.2, and analysis of differential gene expression was conducted using DESeq2 version  
378 1.32.0. Reported genes had a 2-fold-higher or -lower abundance than the wild type, all with an  
379 adjusted p-value of 0.05 or lower.

380

### 381 ***70S ribosome purification***

382 70S ribosomes were isolated using sucrose cushion centrifugation essentially as described (57). Briefly,  
383 wild-type *F. tularensis* cells were grown in 500 mL sMHB to mid-log ( $OD_{600}$  0.3-0.4). Cells were chilled  
384 on ice for 20 minutes, centrifuged at 11,000 x g for 5 minutes at 4°C, then washed once with buffer  
385  $H^{10}M^{10}A^{1000}$  (10 mM HEPES KOH pH 7.6, 10 mM  $MgCl_2$ , and 100 mM  $NH_4Cl$ ) to remove ribonucleases.  
386 The pellet was then washed twice with buffer  $H^{10}M^{10}A^{50}$  (10 mM HEPES KOH pH 7.6, 10 mM  $MgCl_2$ , and

387 50 mM NH<sub>4</sub>Cl, with or without 5 mM β-mercaptoethanol [BME]), and resuspended in ~15 mL of  
388 H<sup>10</sup>M<sup>10</sup>A<sup>50</sup> with 20 U Dnase I. Cells were lysed by passing through a French press three times at 800 psi  
389 and cell debris were removed by centrifugation at 146,000 x g for 15 minutes at 4°C. Supernatant was  
390 incubated with 0.5% Brij58 for 30 minutes and layered on top of H<sup>10</sup>M<sup>10</sup>A<sup>500</sup> + 20% sucrose (10 mM  
391 HEPES KOH pH 7.6, 10 mM MgCl<sub>2</sub>, 500 mM NH<sub>4</sub>Cl, 20% sucrose, with or without 5 mM BME).  
392 Ribosomes were pelleted by ultracentrifugation in 70 Ti rotor for 4 hours at 146,000 x g at 4°C. The  
393 pellet was washed twice with H<sup>10</sup>M<sup>10</sup>A<sup>50</sup> and gently resuspended in H<sup>10</sup>M<sup>10</sup>A<sup>50</sup>. This suspension was  
394 then layered onto another sucrose cushion (H<sup>10</sup>M<sup>10</sup>A<sup>50</sup> with 40% sucrose) and centrifuged for 14 hours  
395 at 146,000 x g at 4°C to further purify the ribosomes. Purified 70S ribosomes were gently resuspended  
396 in ~250 μL of H<sup>10</sup>M<sup>10</sup>A<sup>50</sup> and stored at -80°C.

397

#### 398 ***LC-MS/MS of purified LVS ribosomes***

399 70S ribosomes from wild-type LVS cells were prepared as described above. Samples were either  
400 purified via gel stacking prior to mass spectrometry analysis or maintained in H<sup>10</sup>M<sup>10</sup>A<sup>50</sup> and delivered  
401 to the Northwestern Proteomics Core. The proteins were in-gel digested or in-solution digested and  
402 liquid chromatography tandem mass spectrometry (LC-MS/MS) analysis was completed based on  
403 internal protocols, matching peptides to the *F. tularensis* LVS proteome (NC\_007880).

404

#### 405 ***DIA mass spectrometry***

406 Cells were collected from mid-log cultures (OD<sub>600</sub> 0.3-0.4) and resuspended in Buffer 1 (20 mM KHEPES  
407 pH 7.9, 50 mM KCl, 0.5 mM DTT) with protease inhibitor tablets (Complete Mini, EDTA-free, Roche).  
408 Cells were lysed by sonication and protein concentration was determined using a BCA protein assay

409 (Pierce). Lysates with concentrations between 620 and 862 µg/mL were used by the University of  
410 Arkansas for Medical Sciences (UAMS) Proteomics Core for analysis. Protein extraction and protease  
411 digestion was completed according to UAMS internal protocols. Data-independent acquisition (DIA)  
412 was completed with the Orbitrap Exploris 480 mass spectrometer.

413

414 ***Polysome purification and sucrose gradient sedimentation***

415 Polysomes were isolated essentially as described (58). *F. tularensis* cells were grown until early log  
416 (OD<sub>600</sub> 0.2-0.25). Liquid cultures were rapidly filtered through 0.2 µm nitrocellulose membranes and  
417 transferred to a conical tube filled with liquid nitrogen. Cells were lysed by bead-beating with 650 µL  
418 flash frozen lysis buffer (25 mM HEPES pH 7.6, 100 mM NH<sub>4</sub>Cl, 10 mM MgCl<sub>2</sub>, 0.4% Triton X-100, 0.1%  
419 NP-40, 100 U/mL Rnase-free Dnase) using the TissueLyser II (Qiagen) five times (15 Hz, 3 mins). Cell  
420 debris was pelleted and the polysome-containing lysates were stored at -80°C.

421

422 Sucrose gradients were prepared using 10 and 55% sucrose solutions in 25 mM HEPES pH 7.6, 100 mM  
423 NH<sub>4</sub>Cl, 10 mM MgCl<sub>2</sub> with the BioComp Instruments 153 Gradient Station (BioComp). Cell lysates were  
424 layered onto gradients and centrifuged with the Beckman-Coulter SW40 Ti rotor at 40,000 rpm for 2.5  
425 hr at 4°C. Gradients were fractionated using the Triax full spectrum flow cell and fractionator  
426 (BioComp; 0.2 mm/s, 28 fractions) and A260 was measured every second. Collected fractions were  
427 stored at -80°C. 20 µL of each fraction was combined with 10 µL of sample loading buffer (3X NuPAGE  
428 LDS with 50 mM DTT) and immunoblotted as described above.

429

430 ***Intramacrophage replication assays***

431 Intramacrophage growth assays were performed as previously described (56). Briefly, approximately  
432  $2.5 \times 10^4$  cells of murine macrophage-like J774A.1 cells were incubated at 37°C in 5% CO<sub>2</sub> overnight in  
433 96-well plates in DMEM (Invitrogen) supplemented with 10% fetal bovine serum (Gemini Bio-Products;  
434 DMEM-F). Macrophage cells were infected with LVS and indicated derivative strains at an MOI of  
435 approximately 5 – 10. After two hours, cells were washed twice with PBS and media was replaced with  
436 DMEM-F containing 10 µg/mL gentamycin. After 2 or 24 hours of infection, macrophage were lysed for  
437 30 minutes in 1% saponin in PBS and plated for enumeration.

438

439 ***Antibiotic chase experiment***

440 Indicated *F. tularensis* LVS cells were grown to mid-log in liquid culture (OD<sub>600</sub> 0.3-0.4). Spectinomycin  
441 was added to a final concentration of 200 µg/mL. Cells were collected at the indicated time points after  
442 antibiotic addition and resuspended in sample loading buffer normalized to OD<sub>600</sub> at t=0.  
443 Immunoblotting was conducted as described above and analysis was conducted using one-phase decay  
444 equation on Prism 9 (GraphPad). Data represents two experiments in biological triplicate.

445

446 ***Data availability***

447 RNA-Seq reads are available in the National Center for Biotechnology Information Gene Expression  
448 Omnibus (NCBI GEO) under accession number GSE210766.

449

450 ***Acknowledgements***

451 For helpful comments on the manuscript, we thank Dr. Simon L. Dove, Dr. Steven T. Gregory, and Dr.  
452 Matthew M. Ramsey. For use of shared equipment, we thank Dr. Gregory, Dr. Jodi L. Camberg, and Dr.  
453 Niall G. Howlett. We thank the other members of the Ramsey laboratory. We also thank Janet Atoyan  
454 and the URI Genomics and Sequencing Center (now Rhode Island INBRE Molecular Informatics Core).

455

456 ***Funding Information***

457 This work was funded by a NIGMS CARTD-COBRE Pilot Project Award (P20GM121344—KMR), a  
458 NIGMS/RI-INBRE Early Career Development Award (P20GM103430—KMR), and a Rhode Island  
459 Foundation Medical Research Grant (2798\_20190602—KMR). This work was supported by the USDA  
460 National Institute of Food and Agriculture, Hatch Formula project accession number 1017848.

461

462 This material is based upon work conducted at a Rhode Island NSF EPSCoR research facility, the  
463 Genomics and Sequencing Center, supported in part by the National Science Foundation EPSCoR  
464 Cooperative Agreements 0554548, EPS-1004057, and OIA-1655221. Research was made possible by  
465 the use of equipment and services available through the Rhode Island Institutional Development  
466 Award (IDeA) Network of Biomedical Research Excellence from the National Institute of General  
467 Medical Sciences of the National Institutes of Health under grant number P20GM103430 through the  
468 Centralized Research Core facility and the Molecular Informatics Core (RRID:SCR\_017685). LC-MS/MS  
469 proteomics were performed by the Northwestern Proteomics Core Facility, supported by NCI CCSG P30  
470 CA060553, instrumentation award (S10OD025194), and the National Resource for Translational and  
471 Developmental Proteomics supported by P41 GM108569. DIA proteomics were performed by IDeA



472 National Resource for Quantitative Proteomics, supported by NIGMS R24GM137786. Antibodies for  
473 the following *Francisella tularensis* proteins were obtained through BEI Resources, NIAID, NIH: PdpB,  
474 IgIA, IgIB, IgIC, and IgID.

475

## 476   **References**

477

- 478    1. Hershey JWB, Sonenberg N, Mathews MB. 2012. Principles of Translational Control: An Overview.  
479    Csh Perspect Biol 4:a011528.
- 480    2. Duval M, Simonetti A, Caldelari I, Marzi S. 2015. Multiple ways to regulate translation initiation in  
481    bacteria: Mechanisms, regulatory circuits, dynamics. Biochimie 114:18–29.
- 482    3. Byrgazov K, Vesper O, Moll I. 2013. Ribosome heterogeneity: another level of complexity in bacterial  
483    translation regulation. Curr Opin Microbiol 16:133–139.
- 484    4. Xue S, Barna M. 2012. Specialized ribosomes: a new frontier in gene regulation and organismal  
485    biology. Nat Rev Mol Cell Bio 13:355–69.
- 486    5. Kurylo CM, Parks MM, Juetten MF, Zinshteyn B, Altman RB, Thibado JK, Vincent CT, Blanchard SC.  
487    2018. Endogenous rRNA Sequence Variation Can Regulate Stress Response Gene Expression and  
488    Phenotype. Cell Reports 25:236-248.e6.
- 489    6. Song W, Joo M, Yeom J-H, Shin E, Lee M, Choi H-K, Hwang J, Kim Y-I, Seo R, Lee JE, Moore CJ, Kim Y-  
490    H, Eyun S-I, Hahn Y, Bae J, Lee K. 2019. Divergent rRNAs as regulators of gene expression at the  
491    ribosome level. Nat Microbiol 4:515–526.
- 492    7. Chen Y-X, Xu Z, Ge X, Hong J-Y, Sanyal S, Lu ZJ, Javid B. 2020. Selective translation by alternative  
493    bacterial ribosomes. Proc National Acad Sci 117:19487–19496.

- 494 8. Sjöstedt A. 2007. Tularemia: History, Epidemiology, Pathogen Physiology, and Clinical  
495 Manifestations. *Ann Ny Acad Sci* 1105:1–29.
- 496 9. Barker JR, Chong A, Wehrly TD, Yu J-J, Rodriguez SA, Liu J, Celli J, Arulanandam BP, Klose KE. 2009.  
497 The *Francisella tularensis* pathogenicity island encodes a secretion system that is required for  
498 phagosome escape and virulence. *Molecular Microbiology* 74:1459–1470.
- 499 10. Bröms JE, Meyer L, Sun K, Lavander M, Sjöstedt A. 2012. Unique substrates secreted by the type VI  
500 secretion system of *Francisella tularensis* during intramacrophage infection. *PLoS ONE* 7:e50473.
- 501 11. Eshraghi A, Kim J, Walls AC, Ledvina HE, Miller CN, Ramsey KM, Whitney JC, Radey MC, Peterson SB,  
502 Ruhland BR, Tran BQ, Goo YA, Goodlett DR, Dove SL, Celli J, Veessler D, Mougous JD. 2016. Secreted  
503 Effectors Encoded within and outside of the Francisella Pathogenicity Island Promote Intramacrophage  
504 Growth. *Cell Host Microbe* 20:573–583.
- 505 12. Ledvina HE, Kelly KA, Eshraghi A, Plemel RL, Peterson SB, Lee B, Steele S, Adler M, Kawula TH, Merz  
506 AJ, Skerrett SJ, Celli J, Mougous JD. 2018. A Phosphatidylinositol 3-Kinase Effector Alters Phagosomal  
507 Maturation to Promote Intracellular Growth of *Francisella*. *Cell Host Microbe* 24:285-295.e8.
- 508 13. Lauriano CM, Barker JR, Yoon S-S, Nano FE, Arulanandam BP, Hassett DJ, Klose KE. 2004. MglA  
509 regulates transcription of virulence factors necessary for *Francisella tularensis* intraamoebae and  
510 intramacrophage survival. *Proc National Acad Sci* 101:4246–4249.

- 511 14. Charity JC, Costante-Hamm MM, Balon EL, Boyd DH, Rubin EJ, Dove SL. 2007. Twin RNA  
512 polymerase-associated proteins control virulence gene expression in *Francisella tularensis*. PLoS  
513 Pathog 3:e84.
- 514 15. Charity JC, Blalock LT, Costante-Hamm MM, Kasper DL, Dove SL. 2009. Small molecule control of  
515 virulence gene expression in *Francisella tularensis*. PLoS Pathog 5:e1000641.
- 516 16. Brotcke A, Monack DM. 2008. Identification of *fevR*, a novel regulator of virulence gene expression  
517 in *Francisella novicida*. Infect Immun 76:3473–3480.
- 518 17. Rohlfing AE, Dove SL. 2014. Coordinate control of virulence gene expression in *Francisella tularensis*  
519 involves direct interaction between key regulators. J Bacteriol 196:3516–3526.
- 520 18. Ramsey KM, Osborne ML, Vvedenskaya IO, Su C, Nickels BE, Dove SL. 2015. Ubiquitous promoter-  
521 localization of essential virulence regulators in *Francisella tularensis*. Plos Pathog 11:e1004793.
- 522 19. Cuthbert BJ, Ross W, Rohlfing AE, Dove SL, Gourse RL, Brennan RG, Schumacher MA. 2017.  
523 Dissection of the molecular circuitry controlling virulence in *Francisella tularensis*. Genes Dev 31:1549–  
524 1560.
- 525 20. Travis BA, Ramsey KM, Prezioso SM, Tallo T, Wandzilak JM, Hsu A, Borgnia M, Bartesaghi A, Dove  
526 SL, Brennan RG, Schumacher MA. 2021. Structural Basis for Virulence Activation of *Francisella*  
527 *tularensis*. Mol Cell 81:139-152.e10.
- 528 21. Duin JV, Wijnands R. 1981. The function of ribosomal protein S21 in protein synthesis. Eur J  
529 Biochem 118:615–9.

- 530 22. Chang C, Craven GR. 1977. Identification of several proteins involved in the messenger RNA binding  
531 site of the 30 S ribosome by inactivation with 2-methoxy-5-nitro tropone. J Mol Biol 117:401–18.
- 532 23. Berk V, Zhang W, Pai RD, Cate JHD. 2006. Structural basis for mRNA and tRNA positioning on the  
533 ribosome. Proc Natl Acad Sci U S A 103:15830–15834.
- 534 24. Watson ZL, Ward FR, Méheust R, Ad O, Schepartz A, Banfield JF, Cate JH. 2020. Structure of the  
535 bacterial ribosome at 2 Å resolution. Elife 9:e60482.
- 536 25. Mizushima S, Nomura M. 1970. Assembly Mapping of 30S Ribosomal Proteins from *E. coli*. Nature  
537 226:1214–1218.
- 538 26. Robertson WR, Dowsett SJ, Hardy SJS. 1977. Exchange of ribosomal proteins among the ribosomes  
539 of *Escherichia coli*. Mol Gen Genet 157:205–214.
- 540 27. Lupski JR, Godson GN. 1984. The *rpsU-dnaG-rpoD* macromolecular synthesis operon of *E. coli*. Cell  
541 39:251–252.
- 542 28. Deniziak M, Sauter C, Becker HD, Paulus CA, Giegé R, Kern D. 2007. Deinococcus glutaminyl-tRNA  
543 synthetase is a chimera between proteins from an ancient and the modern pathways of aminoacyl-tRNA  
544 formation. Nucleic Acids Res 35:1421–1431.
- 545 29. Searle BC, Swearingen KE, Barnes CA, Schmidt T, Gessulat S, Küster B, Wilhelm M. 2020. Generating  
546 high quality libraries for DIA MS with empirically corrected peptide predictions. Nat Commun 11:1548.

- 547 30. Takata R. 1978. Genetic studies of the ribosomal proteins in *Escherichia coli* XI. Mol Gen Genetics  
548 Mgg 160:151–155.
- 549 31. Nomura M, Gourse R, Baughman G. 1984. Regulation of the Synthesis of Ribosomes and Ribosomal  
550 Components. Annu Rev Biochem 53:75–117.
- 551 32. Nano FE, Zhang N, Cowley SC, Klose KE, Cheung KKM, Roberts MJ, Ludu JS, Letendre GW,  
552 Meierovics AI, Stephens G, Elkins KL. 2004. A *Francisella tularensis* Pathogenicity Island Required for  
553 Intramacrophage Growth. J Bacteriol 186:6430–6436.
- 554 33. Larsson P, Oyston PCF, Chain P, Chu MC, Duffield M, Fuxelius H-H, Garcia E, Hälltorp G, Johansson  
555 D, Isherwood KE, Karp PD, Larsson E, Liu Y, Michell S, Prior J, Prior R, Malfatti S, Sjöstedt A, Svensson K,  
556 Thompson N, Vergez L, Wagg JK, Wren BW, Lindler LE, Andersson SGE, Forsman M, Titball RW. 2005.  
557 The complete genome sequence of *Francisella tularensis*, the causative agent of tularemia. Nat Genet  
558 37:153–159.
- 559 34. Nano FE, Schmerk C. 2007. The *Francisella* Pathogenicity Island. Ann Ny Acad Sci 1105:122–137.
- 560 35. Brotcke A, Weiss DS, Kim CC, Chain P, Malfatti S, Garcia E, Monack DM. 2006. Identification of  
561 MglA-regulated genes reveals novel virulence factors in *Francisella tularensis*. Infect Immun 74:6642–  
562 6655.
- 563 36. Vargas-Blanco DA, Shell SS. 2020. Regulation of mRNA Stability During Bacterial Stress Responses.  
564 Front Microbiol 11:2111.

- 565 37. Yutin N, Puigbo P, Koonin EV, Wolf YI. 2012. Phylogenomics of prokaryotic ribosomal proteins. Plos  
566 One 7:e36972.
- 567 38. Galperin MY, Wolf YI, Garushyants SK, Alvarez RV, Koonin EV. 2021. Nonessential Ribosomal  
568 Proteins in Bacteria and Archaea Identified Using Clusters of Orthologous Genes. J Bacteriol 203.
- 569 39. Bubunenko M, Baker T, Court DL. 2007. Essentiality of ribosomal and transcription antitermination  
570 proteins analyzed by systematic gene replacement in *Escherichia coli*. J Bacteriol 189:2844–2853.
- 571 40. Yamamoto N, Nakahigashi K, Nakamichi T, Yoshino M, Takai Y, Touda Y, Furubayashi A, Kinjyo S,  
572 Dose H, Hasegawa M, Datsenko KA, Nakayashiki T, Tomita M, Wanner BL, Mori H. 2009. Update on the  
573 Keio collection of *Escherichia coli* single-gene deletion mutants. Mol Syst Biol 5:335.
- 574 41. Goodall ECA, Robinson A, Johnston IG, Jabbari S, Turner KA, Cunningham AF, Lund PA, Cole JA,  
575 Henderson IR. 2018. The Essential Genome of *Escherichia coli* K-12. mBio 9:e02096-17.
- 576 42. Ramsey KM, Ledvina HE, Tresko TM, Wandzilak JM, Tower CA, Tallo T, Schramm CE, Peterson SB,  
577 Skerrett SJ, Mougous JD, Dove SL. 2020. Tn-Seq reveals hidden complexity in the utilization of host-  
578 derived glutathione in *Francisella tularensis*. Plos Pathog 16:e1008566.
- 579 43. Jha V, Roy B, Jahagirdar D, McNutt ZA, Shatoff EA, Boleratz BL, Watkins DE, Bundschuh R, Basu K,  
580 Ortega J, Fredrick K. 2020. Structural basis of sequestration of the anti-Shine-Dalgarno sequence in the  
581 Bacteroidetes ribosome. Nucleic Acids Res 49:547–567.

- 582 44. Takada H, Morita M, Shiwa Y, Sugimoto R, Suzuki S, Kawamura F, Yoshikawa H. 2014. Cell motility  
583 and biofilm formation in *Bacillus subtilis* are affected by the ribosomal proteins, S11 and S21. Biosci  
584 Biotechnology Biochem 78:898–907.
- 585 45. Metselaar KI, Besten HMW den, Boekhorst J, Hijum SAFT van, Zwietering MH, Abee T. 2015.  
586 Diversity of acid stress resistant variants of *Listeria monocytogenes* and the potential role of ribosomal  
587 protein S21 encoded by *rpsU*. Front Microbiol 6:422.
- 588 46. Metselaar KI, Abee T, Zwietering MH, Besten HMW den. 2016. Modeling and Validation of the  
589 Ecological Behavior of Wild-Type *Listeria monocytogenes* and Stress-Resistant Variants. Appl Environ  
590 Microb 82:5389–5401.
- 591 47. Basco MDS, Kothari A, McKinzie PB, Revollo JR, Agnihothram S, Azevedo MP, Saccente M, Hart ME.  
592 2019. Reduced vancomycin susceptibility and increased macrophage survival in *Staphylococcus aureus*  
593 strains sequentially isolated from a bacteraemic patient during a short course of antibiotic therapy. J  
594 Med Microbiol 68:848–859.
- 595 48. Blake KL, O'Neill AJ. 2013. Transposon library screening for identification of genetic loci  
596 participating in intrinsic susceptibility and acquired resistance to antistaphylococcal agents. J  
597 Antimicrob Chemother 68:12–16.
- 598 49. Friedman L, Alder JD, Silverman JA. 2006. Genetic Changes That Correlate with Reduced  
599 Susceptibility to Daptomycin in *Staphylococcus aureus*. Antimicrob Agents Chemother 50:2137–2145.



600 50. Gutierrez MG, Yoder-Himes DR, Warawa JM. 2015. Comprehensive identification of virulence  
601 factors required for respiratory melioidosis using Tn-seq mutagenesis. *Front Cell Infect Microbiol* 5:78.

602 51. Su J, Yang J, Zhao D, Kawula TH, Banas JA, Zhang J-R. 2007. Genome-Wide Identification of  
603 *Francisella tularensis* Virulence Determinants. *Infect Immun* 75:3089–3101.

604 52. Mizuno CM, Guyomar C, Roux S, Lavigne R, Rodriguez-Valera F, Sullivan MB, Gillet R, Forterre P,  
605 Krupovic M. 2019. Numerous cultivated and uncultivated viruses encode ribosomal proteins. *Nat*  
606 *Commun* 10:752.

607 53. Al-Shayeb B, Sachdeva R, Chen L-X, Ward F, Munk P, Devoto A, Castelle CJ, Olm MR, Bouma-  
608 Gregson K, Amano Y, He C, Méheust R, Brooks B, Thomas A, Lavy A, Matheus-Carnevali P, Sun C,  
609 Goltsman DSA, Borton MA, Sharrar A, Jaffe AL, Nelson TC, Kantor R, Keren R, Lane KR, Farag IF, Lei S,  
610 Finstad K, Amundson R, Anantharaman K, Zhou J, Probst AJ, Power ME, Tringe SG, Li W-J, Wrighton K,  
611 Harrison S, Morowitz M, Relman DA, Doudna JA, Lehours A-C, Warren L, Cate JHD, Santini JM, Banfield  
612 JF. 2020. Clades of huge phages from across Earth’s ecosystems. *Nature* 578:425–431.

613 54. Chen L-X, Jaffe AL, Borges AL, Penev PI, Nelson TC, Warren LA, Banfield JF. 2022. Phage-encoded  
614 ribosomal protein S21 expression is linked to late-stage phage replication. *Isme Commun* 2:31.

615 55. Maier TM, Havig A, Casey M, Nano FE, Frank DW, Zahrt TC. 2004. Construction and Characterization  
616 of a Highly Efficient *Francisella* Shuttle Plasmid. *Appl Environ Microbiol* 70:7511–7519.

617 56. Ramsey KM, Dove SL. 2016. A response regulator promotes *Francisella tularensis* intramacrophage  
618 growth by repressing an anti-virulence factor. *Mol Microbiol* 101:688–700.

619 57. Skeggs PA, Thompson J, Cundliffe E. 1985. Methylation of 16S ribosomal RNA and resistance to  
620 aminoglycoside antibiotics in clones of *Streptomyces lividans* carrying DNA from *Streptomyces*  
621 *tenjimariensis*. Mol Gen Genet 200:415–421.

622 58. Johnson GE, Li G-W. 2018. Genome-Wide Quantitation of Protein Synthesis Rates in Bacteria.  
623 Methods Enzymol 612:225–249.

624

625 **FIGURES**

626

627 **Figure 1. *F. tularensis* ribosomes are heterogenous with respect to bS21.** **A.** Chart demonstrating  
628 purity of wild-type ribosomes. Categories represent classification of proteins identified by mass  
629 spectrometry of ribosomes purified from wild-type *F. tularensis* LVS cells. Numbers represent the  
630 percentage of spectral counts corresponding to proteins in each category, combined from  
631 quadruplicate samples. **B.** Wild-type *F. tularensis* LVS ribosomes contain more than one bS21 homolog.  
632 Table detailing the number of spectral counts corresponding to bS21 homologs identified from  
633 individual ribosome purifications (A – D) from wild-type cells. Spectral counts corresponding to bS21-1  
634 and/or bS21-3 cannot be unambiguously assigned due to complete sequence identity of detected  
635 peptides. ND: not detected. **C.** Each bS21 homolog can be incorporated into ribosomes. Top: Sucrose  
636 gradient sedimentation profile from actively-translating wild-type cells containing an empty vector.  
637 Nucleic acid content was monitored by A260 (y-axis). Peaks corresponding to the 30S, 50S, 70S, and  
638 polysomes are indicated. Fractions collected are indicated on the x-axis. Bottom: Immunoblot analysis  
639 of fractions from sucrose gradient sedimentation performed on actively-translating cells ectopically  
640 expressing indicated bS21 homolog with VSV-G epitope tag. Wells correspond to fractions 1 – 21 from  
641 profile above.

642

643 **Figure 2. Loss of bS21-2 leads to changes in protein abundance that cannot be explained by changes**  
644 **in transcript abundance.** Cells with (WT, wild-type) and without bS21-2 ( $\Delta rpsU2$ ) were analyzed using  
645 RNA-Seq (x-axis) and DIA whole cell mass spectrometry (y-axis). Genes are represented by dots. Most  
646 genes with changes in protein (161 yellow dots) do not have corresponding changes in transcript  
647 abundance. One gene (orange dot) has discordant changes in transcript and protein abundance. Green

648 dots (23) represent genes with concordant changes in transcript and protein abundance. Blue dots (60)  
649 indicate genes with altered transcript abundance only. Horizontal dashed lines indicate +/- 1.5-fold  
650 cutoff for differential protein abundance; vertical dashes indicate +/- 2-fold cutoff for differential  
651 transcript abundance. Colored dots with black outlines represent genes with significant changes in  
652 protein (+/- 1.5-fold change, adjusted p-value <0.05) and/or transcript (+/- 2-fold change, adjusted p-  
653 value <0.05) abundance as indicated above, while grey dots without outline represent genes with  
654 changes that did not meet the statistical thresholds. Three grey dots are located outside the bounds of  
655 the axis as represented.

656

657 **Figure 3. bS21-2 impacts T6SS protein abundance. A.** Immunoblot analysis of indicated T6SS protein  
658 abundance. Cells either contained (wild-type) or lacked ( $\Delta rpsU2$ ) bS21-2 and either an empty vector  
659 control (pF) or a vector ectopically expressing VSV-G-tagged bS21 homologs (pF-bS21-1-V, pF-bS21-2-V,  
660 or pF-bS21-3-V). Immunoblot against VSV-G was included to demonstrate production of VSV-G-tagged  
661 bS21 homologs. **B.** Quantification of immunoblots from (A). Band intensities for each protein were  
662 normalized to total protein per well on the membrane. Error bars represent 1 SD. Experiments were  
663 repeated at least twice and data from a representative experiment are shown. Lines above bars  
664 indicate statistical comparison among groups by t-test. Asterisk indicates group to which all other  
665 groups are compared, if horizontal line connects to line above group,  $*p < 0.05$  using Benjamini-  
666 Hochberg correction.

667

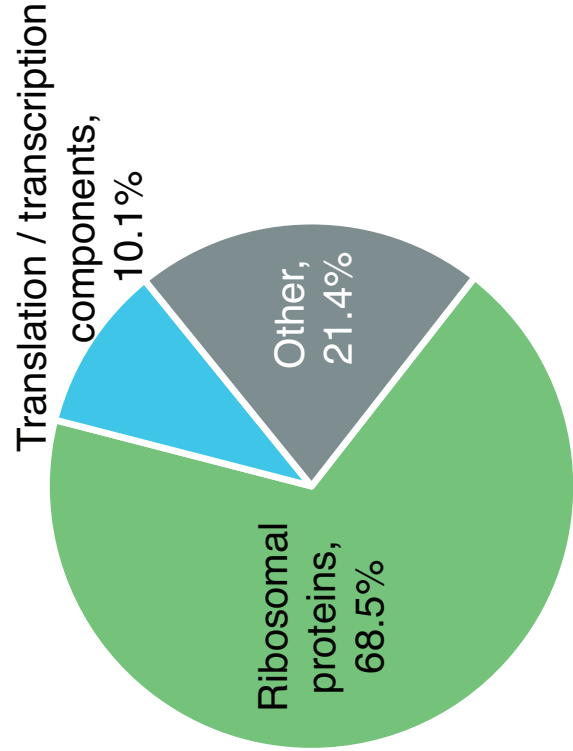
668 **Figure 4. Cells without bS21-2 have an intramacrophage growth defect, which can be complemented**  
669 **by ectopic expression of bS21-2.** Growth and survival of *F. tularensis* LVS cells within J774A.1 cells.

670 Murine macrophage-like J774A.1 cells were infected with indicated bacterial cells at a multiplicity of  
671 infection of 5 – 10. J774A.1 cells were lysed and bacteria were plated for enumeration (colony forming  
672 units [CFU]) at 2- and 24-hours post-infection. Error bars represent 1 SD. Experiments were repeated at  
673 least twice and data from a representative experiment are shown. Lines above bars indicate statistical  
674 comparison among groups by t-test. Asterisk indicates group to which all other groups are compared, if  
675 horizontal line connects to line above group,  $*p < 0.05$  using Benjamini-Hochberg correction.

676

677

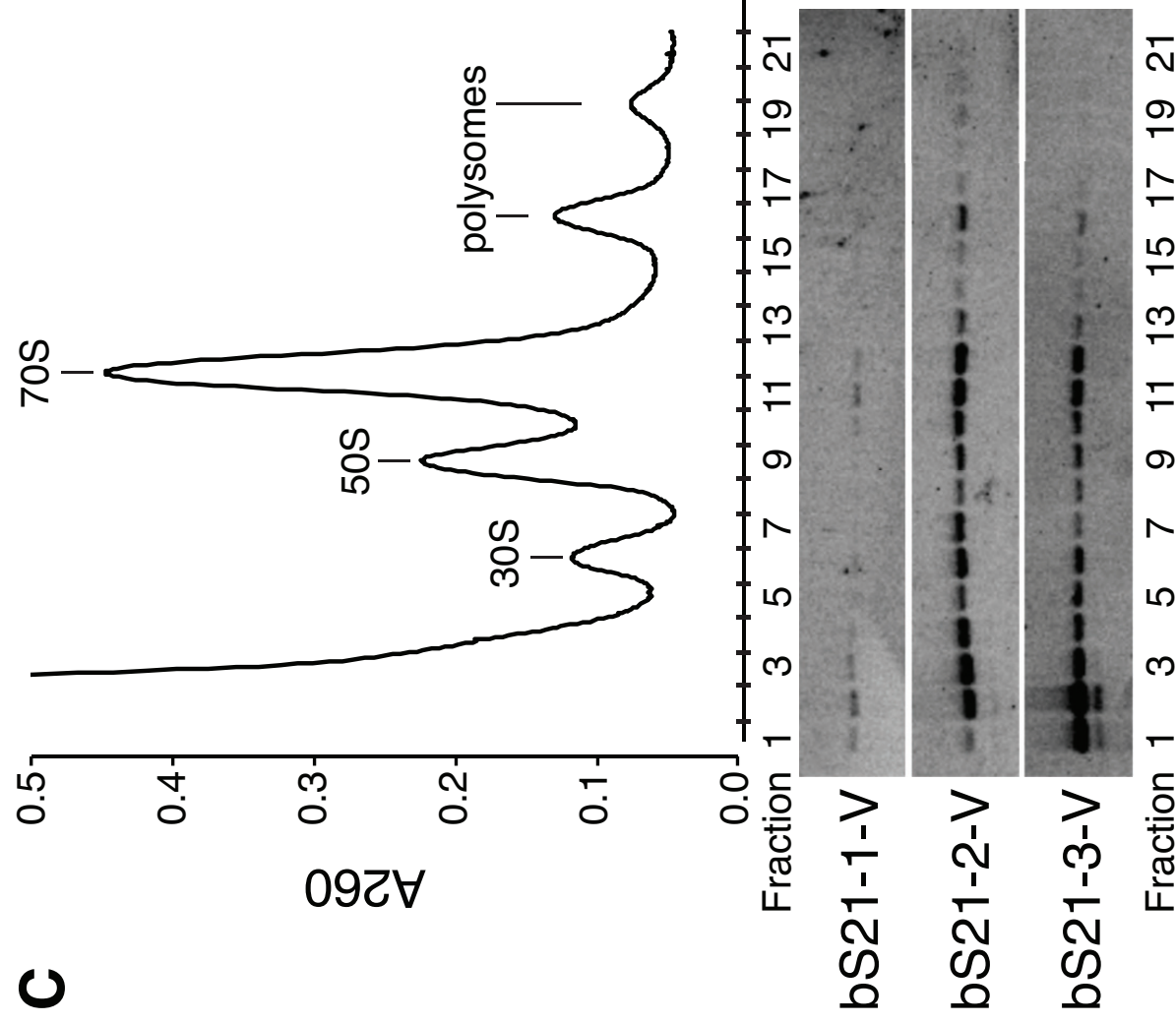
**A**

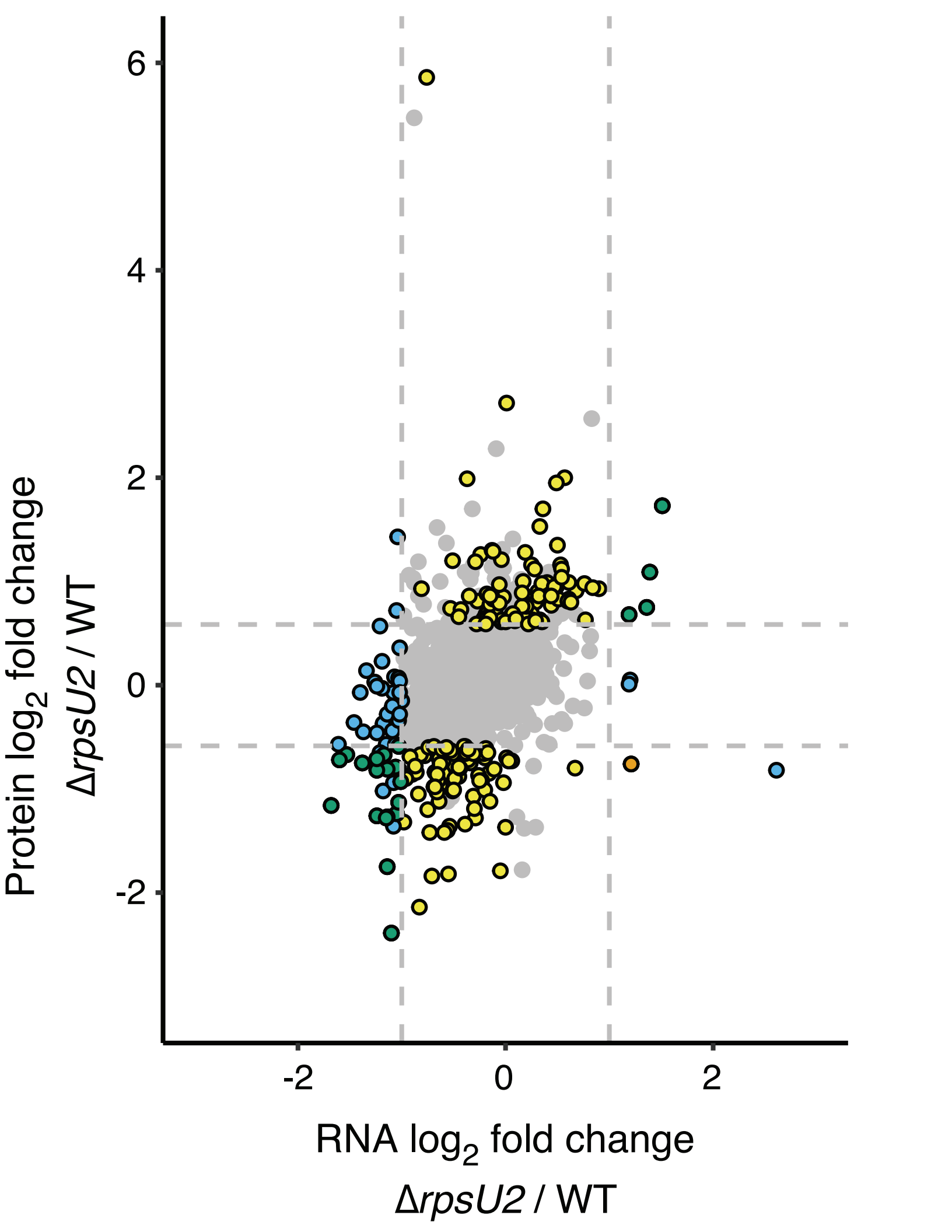


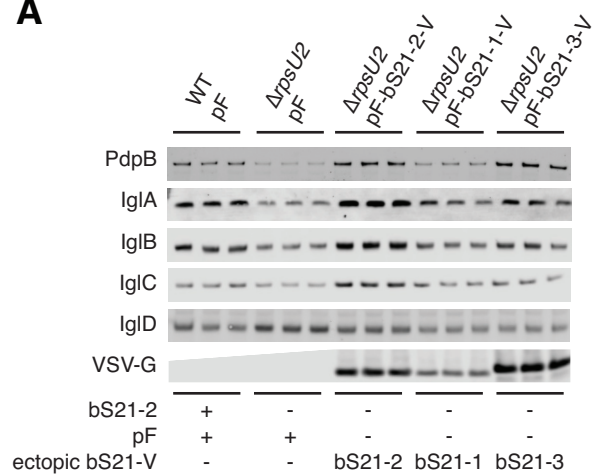
**B**

Peptides corresponding to	Spectral counts			
	A	B	C	D
bS21-2	18	11	8	9
bS21-1 and/or bS21-3	3	ND	ND	ND

**C**





**A****B**